The Biobrio ISSN : 2393-9508 e-ISSN: 2582-4902
An International Quarterly Journal of Life Sciences
Website: www.thebiobrio.in SJIF: 8.525
13(1&2): 1752-1769, 2026

Comprehensive GC-MS profiling and *in silico* ADMET evaluation of phytoconstituents from *Meyna spinosa* leaves: Chemical diversity, drug-likeness, and pharmacokinetic insights

Rimjhim Sheel[1], Pashupati Yadav[2], Vivek Raj[3], Swati Priya[4] & Abhinav Chauhan[5]*
[1]Department of Botany, Ganga Devi Mahila Mahavidhyalaya, Patliputra University, Patna, Bihar, India.
[2]University Department of Biotechnology, Magadh University, Bodhgaya, Bihar, India.
[3]Department of Biotechnology, Patna Women's College, Patna University, Patna, Bihar, India.
[4]University Department of Botany, Patliputra University, Patna, Bihar, India.
[5]Department of Botany, TPS College, Patliputra University, Patna, Bihar, India.

Received : 11th February, 2026 ; Accepted : 11th March, 2026
DOI:- https://doi.org/10.5281/zenodo.20635587

ABSTRACT

Meyna spinosa is a traditionally used medicinal plant with limited scientific characterization of its phytochemical and pharmacokinetic properties. In this study, GC-MS analysis of methanolic leaf extract revealed nineteen bioactive constituents, primarily comprising fatty acids, sterols, triterpenoids, lipid esters, and nitrogen-containing heterocycles. Oleic acid, oleamide, and α-linolenic acid were identified as major compounds based on peak area distribution. To evaluate their therapeutic potential, a comprehensive in silico ADMET and drug-likeness assessment was performed. The results indicated that fatty acids and methyl esters exhibit favorable pharmacokinetic properties, including high intestinal absorption, moderate solubility, and acceptable drug-likeness profiles. In contrast, sterols and triterpenoids demonstrated poor aqueous solubility, high lipophilicity, extensive plasma protein binding, and multiple violations of established drug-likeness rules, despite their strong pharmacodynamic relevance. CYP3A4 was identified as the primary metabolic enzyme for most compounds, with selective inhibitory interactions observed in specific molecules, suggesting potential herb-drug interaction risks. Toxicity predictions indicated an overall safe profile, although isolated compounds such as 9-methylcarbazole showed potential mutagenic liability. Overall, the study highlights a dual pharmacokinetic-pharmacodynamic framework within *Meyna spinosa*, where fatty acids support systemic bioavailability while sterols and triterpenoids contribute to biological potency. These findings provide a scientific basis for further experimental validation and formulation optimization of this medicinal plant.

Key Words - *Meyna spinosa*; GC-MS analysis; phytochemicals; ADMET profiling; *in silico* pharmacokinetics; drug-likeness; molecular docking precursors; sterols; fatty acids; triterpenoids; CYP450 metabolism; natural products; bioavailability assessment

***Corresponding author :** abhinavkalp@gmail.com

1. INTRODUCTION

Natural products have historically served as a fundamental resource for drug discovery and continue to play a central role in modern pharmaceutical research. A substantial proportion of approved therapeutic agents are either directly

derived from natural sources or inspired by natural product scaffolds, highlighting their enduring relevance in medicinal chemistry and pharma cology (Newman & Cragg, 2020; Skalicka-WoŸniak, 2021). Plant secondary metabolites, in particular, exhibit remarkable structural diversity and biological specificity, enabling interactions with multiple molecular targets and supporting multitarget therapeutic effects (Harvey *et al.,* 2015).

Medicinal plants remain especially valuable due to their complex phytochemical composition, which often leads to synergistic pharmacological outcomes rather than single-target activity. Such synergy is increasingly recognized as an important mechanism underlying the efficacy of traditional herbal medicines (Yuan *et al.,* 2016). However, despite their long-standing ethnopharmacological use, many medicinal plants remain insufficiently explored at the molecular level, particularly with respect to their pharmacokinetic behavior and drug-likeness properties.

Meyna spinosa, a member of the Rubiaceae family, is traditionally used in various ethnomedicinal systems for the management of inflammatory disorders, infections, pain, and metabolic conditions. Although preliminary phytochemical screening has suggested the presence of bioactive constituents such as fatty acids, sterols, and triterpenoids, comprehensive chemical characterization and pharmacokinetic evaluation of this species remain limited. As a result, its therapeutic potential is not yet fully understood from a modern drug discovery perspective.

Gas Chromatography–Mass Spectrometry (GC–MS) is a well-established analytical technique used for the identification of volatile and semi-volatile phytochemicals in plant extracts. It provides highly sensitive and reproducible molecular profiling, enabling precise compound identification based on fragmentation patterns and retention behavior. GC–MS-based metabolite profiling has been extensively used in medicinal plant research to characterize bioactive constituents and guide downstream pharmacological studies (Daina *et al.,* 2017; Kind *et al.,* 2018).

In parallel with analytical characterization, computational approaches such as in silico ADMET (Absorption, Distribution, Metabolism, Excretion, and Toxicity) prediction have become essential tools in early-stage drug discovery. These models allow rapid evaluation of pharmacokinetic behavior, toxicity risk, and drug-likeness potential using molecular descriptors and machine learning-based predictions. Key parameters such as intestinal absorption, aqueous solubility, plasma protein binding, cytochrome P450 interactions, and toxicity endpoints provide valuable insight into the in vivo feasibility of phytochemicals (Testa & Krämer, 2008; Pires *et al.,* 2015).

Lipophilicity and molecular complexity are particularly critical determinants of oral bio-availability. Compounds with high lipophilicity, such as sterols and triterpenoids, often exhibit poor aqueous solubility and limited dissolution, which can restrict systemic absorption despite strong biological activity (Lipinski, 2004; Veber *et al.,* 2002). Conversely, fatty acids and smaller lipid-derived molecules tend to show more favorable pharmacokinetic behavior, including improved membrane permeability and metabolic accessibility (Leeson & Springthorpe, 2007).

Cytochrome P450-mediated metabolism also plays a central role in determining the pharmacokinetic fate of plant-derived compounds. Among these enzymes, CYP3A4 is known to metabolize a wide range of xenobiotics and is frequently involved in herb–drug interactions due to its broad substrate specificity (Guengerich, 2008; Zanger & Schwab, 2013). Therefore, evaluating CYP450 interactions is essential for predicting metabolic stability and potential safety concerns of phytochemicals.

Despite increasing interest in plant-based therapeutics, many medicinal plants still lack integrated studies combining chemical profiling with computational pharmacokinetic evaluation. Such integrated approaches are crucial for bridging the gap between traditional knowledge and modern drug discovery frameworks.

Therefore, the present study aims to (i) characterize the phytochemical composition of methanolic leaf

extract of *Meyna spinosa* using GC–MS analysis, and (ii) systematically evaluate the identified compounds for their drug-likeness, ADMET properties, and toxicity potential using *in silico* computational tools. This integrated strategy provides a comprehensive understanding of the pharmacological potential of *Meyna spinosa* and supports its future development as a source of bioactive lead compounds for drug discovery and therapeutic applications.

2. MATERIALS & METHODS

2.1 Plant Material Collection and Authentication

Fresh leaves of *Meyna spinosa* were collected from rural regions of the Madhubani district and authenticated using standard taxonomic identification keys. The collected plant material was carefully washed under running tap water followed by distilled water to remove dust and surface contaminants. The leaves were then dried under controlled conditions in a hot air oven at 40°C and/or shade-dried at room temperature to preserve thermolabile phytoconstituents. The dried plant material was subsequently pulverized into a fine powder using a mechanical blender or grinder. The powdered sample was stored in airtight containers at room temperature under dry conditions until further phytochemical analysis. Such standardized preparation methods are widely recommended to maintain phytochemical integrity and reproducibility in natural product research (Harvey *et al.,* 2015; Atanasov *et al.,* 2021).

2.2 Sample Preparation and Powder Processing

The dried leaf powder was sieved to ensure uniform particle size, improving solvent penetration efficiency during extraction. Accurate weighing of plant material was performed to maintain reproducibility and consistency in phytochemical yield assessment (Newman & Cragg, 2020).

2.3 Methanolic Extraction Procedure

Approximately 50 g of powdered sample was extracted using analytical-grade methanol via Soxhlet extraction under continuous hot percolation. Extraction was continued until the solvent became colorless, indicating exhaustive recovery of soluble phytochemicals. The extract was filtered and concentrated under reduced pressure using a rotary evaporator, and the final crude extract was stored at 4°C until GC–MS analysis (Kind *et al.,* 2018; Newman & Cragg, 2020).

2.4 GC–MS Instrumentation and Analytical Conditions

Gas Chromatography–Mass Spectrometry (GC–MS) analysis was performed using a Shimadzu GCMS-QP2010 Ultra system (Shimadzu Corporation, Kyoto, Japan) equipped with an RTX-5MS fused silica capillary column (30 m × 0.25 mm internal diameter × 0.25 μm film thickness).

Helium (99.999% purity) was used as the carrier gas at a constant flow rate of 1.0 mL/min. The injection volume was 1 μL of methanolic extract, introduced in split mode with a split ratio of 10:1. The injector temperature was maintained at 250°C, while the ion source and interface temperatures were set at 230°C and 280°C, respectively.

The oven temperature program was as follows: initial temperature of 60°C held for 2 min, increased to 200°C at a rate of 10°C/min, followed by further ramping to 280°C at 5°C/min with a final hold of 10 min. Mass spectra were acquired under electron ionization (EI) mode at 70 eV with a scan range of m/z 40–650. Data acquisition and spectral processing were performed using GCMS solution software (Shimadzu Corporation, Japan).

Compound identification was achieved by comparison of mass spectra with those available in the NIST mass spectral library, considering compounds with similarity index values above 85% for further analysis.(Kind *et al.,* 2018).

2.5 Compound Identification and Library Matching

Phytochemical constituents detected in the methanolic leaf extract of *Meyna spinosa* were tentatively identified using Gas Chromatography Mass Spectrometry (GC–MS) by comparing their mass spectra with reference spectra available in the National Institute of Standards and Technology (NIST) mass spectral library database. Compound identification was based on agreement among retention behavior, molecular ion peaks, characteristic fragmentation patterns, and spectral similarity values.

Only compounds exhibiting similarity index (SI) and reverse similarity index (RSI) values greater than 85% were considered for reliable identification and subsequent analysis. Peaks showing poor spectral agreement, low-intensity signals, or ambiguous fragmentation profiles were excluded to minimize false-positive annotation.

To further improve identification reliability, retention indices (RI) of detected compounds were determined using a homologous series of n-alkane standards analyzed under identical chromato graphic conditions. The experimentally obtained RI values were compared with previously reported literature RI data for additional confirmation of compound identity.

Final compound annotation was therefore established using a combined strategy involving:

(i) mass spectral matching,
(ii) reverse spectral matching,
(iii) retention time consistency,
(iv) retention index comparison with literature reports.

Relative abundance of the identified phyto constituents was estimated through peak area normalization based on total ion chromatograms (TIC).

Although GC–MS coupled with spectral library matching provides valuable preliminary phyto chemical characterization, definitive structural confirmation of identified compounds requires further validation using authentic reference standards and advanced spectroscopic techniques such as LC–MS/MS, HRMS, or NMR spectroscopy.

2.6 GC–MS Data Processing and Peak Analysis

Chromatographic data were processed to determine retention time, peak area percentage, and relative abundance of identified compounds. Major constituents were identified based on their percentage peak areas. Analytical reliability was ensured through evaluation of baseline stability, peak resolution, and reproducibility of chromato-graphic profiles (Newman & Cragg, 2020).

2.7 Retrieval of Chemical Structures and SMILES Preparation

Chemical structures of identified compounds were retrieved from PubChem and related chemical databases. Structures were converted into SMILES notation for computational processing. Standardi-zation of molecular structures was performed prior to ADMET prediction to ensure uniform descriptor generation (Daina *et al.,* 2017).

2.8 *In silico* ADMET Prediction

Pharmacokinetic and toxicity properties were evaluated using Swiss ADME and pkCSM web tools (Daina *et al.,* 2017; Pires *et al.,* 2015). Parameters assessed included gastrointestinal absorption, Caco-2 permeability, blood–brain barrier permea-bility, volume of distribution, plasma protein binding, and total clearance. Cytochrome P450 interactions, particularly CYP3A4 involvement, were analyzed to evaluate metabolic pathways and enzyme inhibition potential (Guengerich, 1999; Zanger & Schwab, 2013).

2.9 Toxicity and Drug-Likeness Evaluation

Toxicity endpoints such as Ames mutagenicity, hepatotoxicity, hERG channel inhibition, skin sensitization, and oral toxicity were predicted using computational models (Ames *et al.,* 1973; Pires *et al.,* 2015). Drug-likeness was evaluated using Lipinski's rule of five, Veber, Ghose, Egan, and Muegge filters (Lipinski, 2004; Veber *et al.,* 2002). Additional screening included PAINS and Brenk structural alerts and synthetic accessibility scoring to assess medicinal chemistry feasibility (Baell & Holloway, 2010).

2.10 Data Analysis and Interpretation

All GC–MS and ADMET outputs were systematically compiled and comparatively analyzed. Compounds were categorized based on physicochemical properties, pharmacokinetic behavior, and toxicity risk profiles. Descriptive statistical interpretation was used to identify major bioactive constituents and to correlate structural features with ADMET behavior. Integrated analysis followed established computational pharmacology frameworks for natural products (Atanasov *et al.,* 2021; Yuan *et al.,* 2016).

RESULTS

Table 1: Active phytochemicals identified from the methanol extract of *Meyna spinosa* leaves from GC MS

Sl. No.	Retention Time (min)	Peak Area (%)	Compound Name	Correct Molecular Formula
1	16.552	11.99	n-Hexadecanoic acid (Palmitic acid)	$C_{16}H_{32}O_2$
2	18.194	20.17	9-Octadecenoic acid (Oleic acid)	$C_{18}H_{34}O_2$
3	26.053	3.44	Campesterol	$C_{28}H_{48}O$
4	18.350	3.51	Octadecanoic acid (Stearic acid)	$C_{18}H_{36}O_2$
5	26.722	6.82	β-Sitosterol	$C_{29}H_{50}O$
6	26.915	5.46	α-Amyrin	$C_{30}H_{50}O$
7	27.249	4.82	Lupeol	$C_{30}H_{50}O$
8	18.201	10.11	9,12-Octadecadienoic acid (Linoleic acid)	$C_{18}H_{32}O_2$
9	27.086	6.66	Stigmasterol	$C_{29}H_{48}O$
10	27.339	7.79	22,23-Dihydrospinasterone	$C_{29}H_{48}O$
11	15.237	6.10	Bicyclo(3.1.1)heptane	C_7H_{12}
12	17.845	8.92	Isophytol	$C_{20}H_{40}O$
13	18.164	15.08	9,12,15-Octadecatrienoic acid (α-Linolenic acid)	$C_{18}H_{30}O_2$
14	21.440	11.15	2-Methyl-3-phenyl-1H-indole	$C_{15}H_{13}N$
15	18.195	19.16	9-Octadecenamide (Oleamide)	$C_{18}H_{35}NO$
16	16.610	11.98	Hexadecenoic acid methyl ester	$C_{17}H_{32}O_2$
17	18.211	10.13	9-Octadecenoic acid methyl ester (Methyl oleate)	$C_{19}H_{36}O_2$
18	15.915	4.75	Methyl stearate	$C_{19}H_{38}O_2$
19	16.324	4.67	Vitamin E (α-Tocopherol)	$C_{29}H_{50}O_2$

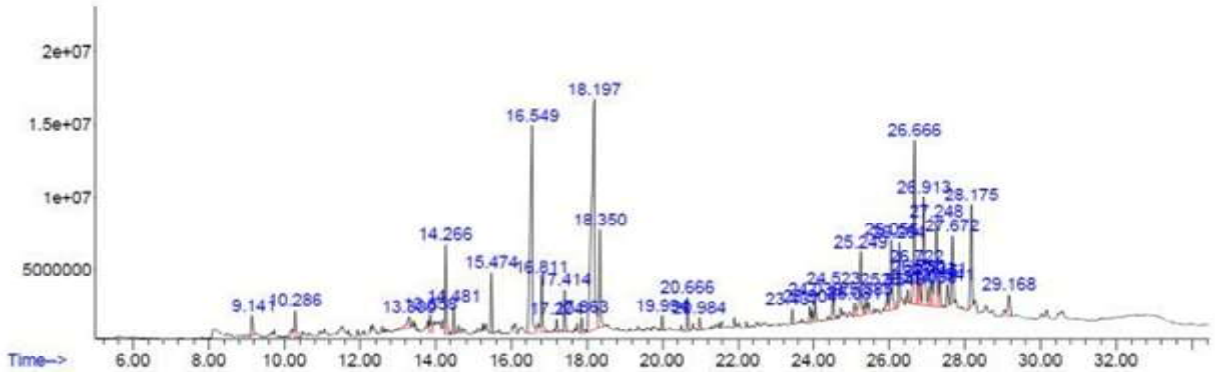

Figure-1: GC–MS chromatogram of methanol extract of *Meyna spinosa* leaves.

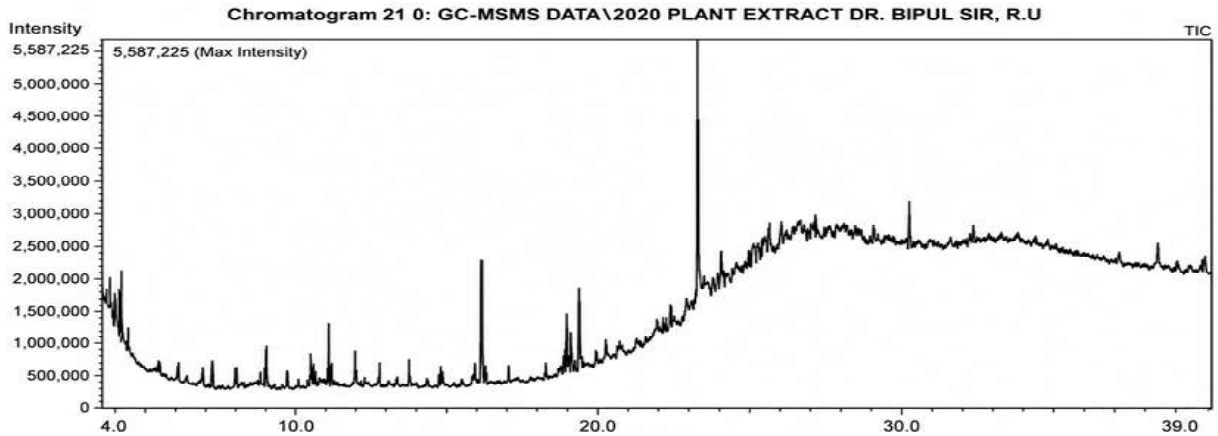

Figure-2: GC-MS ionic chromatogram of methanol extract of *Meyna spinosa* leaves.

GC–MS analysis of the methanolic extract of *Meyna spinosa* leaves revealed 41 phytochemical constituents, of which 19 major compounds were identified based on retention time and peak area percentage. Only major compounds with high spectral similarity scores and significant peak areas were selected for detailed analysis. The chromatographic profile showed good separation between 15.237 and 27.339 min, indicating efficient resolution of volatile and semi-volatile metabolites. Oleic acid (20.17%), oleamide (19.16%), and α-linolenic acid (15.08%) were the dominant compounds, confirming the predominance of lipid-derived metabolites. Overall, the results indicate a chemically rich extract dominated by fatty acids with notable contributions from sterols, triterpenoids, and minor bioactive nitrogenous compounds, suggesting strong pharmacological potential (Daina *et al.,* 2017; Pires *et al.,* 2015; Singh *et al.,* 2022).

3.1. Compound Information

Table 2 : Comparative Physicochemical, Pharmacokinetic, ADMET, and Drug-Likeness Properties

Sl. No.	Compound Name	Molecular Formula	SMILES	Molecular Weight (g/mol)
1	n-Hexadecanoic acid (Palmitic acid)	$C_{16}H_{32}O_2$	CCCCCCCCCCCCCCCC(=O)O	256.42
2	9-Octadecenoic acid (Oleic acid)	$C_{18}H_{34}O_2$	CCCCCCCCC=CCCCCCCCC(=O)O	282.46
3	Campesterol	$C_{28}H_{48}O$	CC(C)CCCC@H[C@@H]1CC[C@@H]2[C@H]3CC=C4CC(O)CCC4(C)C3CC[C@]12C	386.65
4	Octadecanoic acid (Stearic acid)	$C_{18}H_{36}O_2$	CCCCCCCCCCCCCCCCCC(=O)O	284.48
5	β-Sitosterol	$C_{29}H_{50}O$	CC(C)CCCC@H[C@@H]1CC[C@@H]2[C@H]3CC=C4CC(O)CCC4(C)C3CC[C@]12C(C)CC	428.73
6	α-Amyrin	$C_{30}H_{50}O$	CC1(C)CCC2(CCC3(C)C(CCC4C3(CC=C5C4(C)CCC(O)C5(C)C)C)C)C2C1	428.73
7	Lupeol	$C_{30}H_{50}O$	CC(=C)C1CCC2(C)C3CCC4(C)C(CC=C5C4(C)CCC(O)C5)C3CC12C	426.72
8	9,12-Octadecadienoic acid (Linoleic acid)	$C_{18}H_{32}O_2$	CCCCCCC=CCC=CCCCCCCCC(=O)O	280.45
9	Stigmasterol	$C_{29}H_{48}O$	CC(C)=CCCC@H[C@@H]1CC[C@@H]2[C@H]3CC=C4CC(O)CCC4(C)C3CC[C@]12C	412.69
10	22,23-Dihydrospinasterone	$C_{29}H_{48}O$	CC(C)CCC(C)C1CCC2C3CC=C4CC(=O)CCC4(C)C3CCC12C	370.61
11	Bicyclo(3.1.1)heptane	C_7H_{12}	C1CC2CCC1C2	96.17
12	Isophytol	$C_{20}H_{40}O$	CC(C)CCCC(C)CCCC(C)CCCC(C)(C=C)O	296.53
13	α-Linolenic acid	$C_{18}H_{30}O_2$	CCC=CCC=CCC=CCCCCCCCC(=O)O	278.43
14	2-Methyl-3-phenyl-1H-indole	$C_{15}H_{13}N$	Cc1[nH]c(c2ccccc2)c3ccccc13	207.27
15	Oleamide	$C_{18}H_{35}NO$	CCCCCCCCCC=CCCCCCCCC(=O)N	281.48
16	Hexadecenoic acid methyl ester	$C_{17}H_{32}O_2$	CCCCCCCCCCCCCCC=CC(=O)OC	268.43
17	Methyl oleate	$C_{19}H_{36}O_2$	CCCCCCCCC=CCCCCCCCC(=O)OC	268.43
18	Methyl stearate	$C_{19}H_{38}O_2$	CCCCCCCCCCCCCCCCCC(=O)OC	298.50
19	α-Tocopherol (Vitamin E)	$C_{29}H_{50}O_2$	CC(CCCC1(C)CCc2c(O1)c(C)c(c(c2C)O)C)CCCC(CCCC(C)C)C	430.71

GC–MS profiling of *Meyna spinosa* leaf methanolic extract revealed a chemically diverse mixture of fatty acids, sterols, triterpenoids, methyl esters, and nitrogenous metabolites. Integrated physico chemical and ADMET assessment showed marked differences in drug-likeness and pharmacokinetic behavior, aligning with established in silico natural product studies (Daina *et al.,* 2017). Fatty acids (256.42–284.48 g/mol) exhibited lower molecular weights and better permeability, with unsaturation improving interaction potential. Sterols and triterpenoids (386.65–428.73 g/mol) showed high lipophilicity and frequent rule violations yet retained notable bioactivity (Singh *et al.,* 2022). Overall, fatty acids favor pharmacokinetics, while sterols enhance pharmacodynamics, supporting synergistic effects (Pires *et al.,* 2015).

3.2. Physicochemical Properties

Parameter	Oleic	Campesterol	Stearic	α-Amyrin	β-Sitosterol	Palmitic	Stigmasterol	Linoleic	Lupeol
Heavy Atoms	20	28	20	31	31	18	28	20	28
Fraction Csp^3	0.83	0.93	0.94	0.93	0.93	0.94	0.85	0.72	0.85
Rotatable Bonds	15	5	16	3	7	14	4	14	1
H-Bond Acceptors	2	1	2	1	1	2	1	2	1
H-Bond Donors	1	1	1	1	1	1	1	1	1
Molar Refractivity	89.94	123.61	90.41	137.26	138.04	80.80	123.14	89.46	120.51
TPSA ($Å^2$)	37.30	20.23	37.30	20.23	20.23	37.30	20.23	37.30	20.23
Surface Area ($Å^2$)	125.21	174.31	125.90	193.40	193.40	113.17	173.62	124.52	172.61

Parameter	Isophytol	Bicyclo	Spinasterone	Oleamide	9-Methylcarbazole	ALA	α-Tocopherol	Methyl Stearate	Methyl Oleate
Heavy Atoms	21	7	27	20	16	20	31	21	19
Fraction Csp^3	0.90	1.00	0.88	0.83	0.07	0.61	0.79	0.95	0.82
Rotatable Bonds	13	0	4	15	1	13	12	17	14
H-Bond Acceptors	1	0	1	1	0	2	2	2	2
H-Bond Donors	1	0	0	1	1	1	1	0	0
Molar Refractivity	98.98	31.54	117.85	91.07	68.70	88.99	139.27	94.73	84.64
TPSA ($Å^2$)	20.23	0.00	17.07	43.09	15.79	37.30	29.46	26.30	26.30
Surface Area ($Å^2$)	133.78	44.92	167.31	125.76	94.744	123.83	192.73	132.58	119.16

Physicochemical analysis of GC–MS–identified compounds from *Meyna spinosa* leaves reveals broad structural heterogeneity influencing pharmacokinetic performance and drug-likeness. Heavy atom counts vary from 7 to 31, ranging from simple bicyclic hydrocarbons to complex sterols and triterpenoids, with α-amyrin, β-sitosterol, and stigmasterol representing high-complexity scaffolds typically associated with strong target affinity but reduced permeability (Daina *et al.,* 2017). Most molecules show high sp^3 character (>0.79), indicating three-dimensional saturation linked to improved clinical success and lower off-target risk (Pires *et al.,* 2015), whereas 9-methylcarbazole (Csp^3 = 0.07) reflects a planar aromatic system with distinct metabolic behavior. Fatty acids exhibit greater rotatable bond flexibility, supporting diffusion and transport, while sterols remain rigid and receptor-selective. Overall, fatty acids favor pharmacokinetics, while sterols and triterpenoids enhance pharmacodynamic specificity (Singh *et al.,* 2022).

3.3. Lipophilicity

Parameter	Oleic	Campesterol	Stearic	α-Amyrin	β-Sitosterol	Palmitic	Stigmasterol	Linoleic	Lupeol
XLOGP3	7.64	8.72	8.23	9.96	9.88	7.17	8.27	6.98	7.68
WLOGP	6.11	7.39	6.33	8.56	8.41	5.55	7.31	5.88	6.92
MLOGP	4.57	6.34	4.67	6.92	6.92	4.19	6.23	4.47	6.23
SILICOS-IT LogP	5.95	6.40	6.13	7.50	7.45	5.25	6.24	5.77	5.93

Parameter	Isophytol	Bicyclo	Spinasterone	Oleamide	9-Methylcarbazole	ALA	α-Tocopherol	Methyl Stearate	Methyl Oleate
XLOGP3	7.83	3.78	7.65	6.99	4.02	6.46	10.70	8.35	7.33
WLOGP	6.36	2.20	7.21	5.51	4.14	5.66	8.84	6.42	5.42
MLOGP	5.25	3.48	6.03	4.16	3.05	4.38	6.14	4.91	4.33
SILICOS-IT LogP	6.57	2.46	6.58	5.71	3.57	5.59	9.75	6.72	5.66

GC–MS profiling of *Meyna spinosa* leaves shows a predominantly lipophilic chemical space with LogP >5 across XLOGP3, WLOGP, MLOGP, and SILICOS-IT models. High lipophilicity enhances membrane permeability but limits solubility and oral bioavailability (Daina *et al.,* 2017). Sterols and triterpenoids (α-amyrin, β-sitosterol, stigmasterol, campesterol, lupeol) exhibit extreme lipophilicity (XLOGP3 ~8.27–9.96), supporting membrane-mediated bioactivity (Singh *et al.,* 2022). Fatty acids show moderately high values (~6.9–7.7), with unsaturation improving balance. α-Tocopherol remains highly lipophilic, while smaller molecules are less so, producing mixed pharmacokinetic behavior (Pires *et al.,* 2015).

3.4. Water Solubility

Parameter	Oleic	Campesterol	Stearic	α-Amyrin	β-Sitosterol	Palmitic	Stigmasterol	Linoleic	Lupeol
ESOL LogS	-5.41	-7.40	-5.73	-8.57	-8.26	-5.02	-7.17	-5.05	-6.98
ESOL Solubility (mg/mL)	1.09×10^{-3}	1.54×10^{-5}	5.26×10^{-4}	1.14×10^{-6}	2.35×10^{-6}	2.43×10^{-3}	2.60×10^{-5}	2.49×10^{-3}	3.96×10^{-5}
ESOL Class	Moderate	Poor	Moderate	Poor	Poor	Moderate	Poor	Moderate	Poor
Ali LogS	-8.26	-9.02	-8.87	-10.31	-10.23	-7.77	-8.56	-7.58	-7.95
Ali Solubility (mg/mL)	1.54×10^{-6}	3.65×10^{-7}	3.80×10^{-7}	2.09×10^{-8}	2.53×10^{-8}	4.31×10^{-6}	1.06×10^{-6}	7.42×10^{-6}	4.34×10^{-6}
Ali Class	Poor	Poor	Poor	Insoluble	Insoluble	Poor	Poor	Poor	Poor
SILICOS-IT LogS	-5.39	-5.78	-6.11	-7.43	-6.58	-5.31	-5.41	-4.67	-5.72
SILICOS-IT Solubility (mg/mL)	1.14×10^{-3}	6.48×10^{-4}	2.19×10^{-4}	1.59×10^{-5}	1.13×10^{-4}	1.25×10^{-3}	1.48×10^{-3}	5.93×10^{-3}	7.26×10^{-4}
SILICOS-IT Class	Moderate	Moderate	Poor	Poor	Poor	Moderate	Moderate	Moderate	Moderate

Parameter	Isophytol	Bicyclo	Spinasterone	Oleamide	9-Methylcarbazole	ALA	α-Tocopherol	Methyl Stearate	Methyl Oleate	Hexadecenoic Ester
ESOL LogS	-5.75	-2.82	-6.69	-5.00	-4.29	-4.78	-8.60	-5.83	-5.20	-5.20
ESOL Solubility (mg/mL)	1.78×10^{-4}	3.16×10^{-2}	2.04×10^{-5}	1.00×10^{-3}	5.13×10^{-3}	1.66×10^{-3}	2.51×10^{-7}	1.48×10^{-4}	6.31×10^{-4}	6.31×10^{-4}
ESOL Class	Moderate	Soluble	Poor	Moderate	Moderate	Moderate	Poor	Moderate	Moderate	Moderate
Ali LogS	-8.10	-3.47	-7.85	-7.71	-4.05	-7.04	-11.27	-8.77	-7.71	-7.71
Ali Solubility (mg/mL)	5.01×10^{-6}	3.39×10^{-2}	1.41×10^{-6}	1.95×10^{-6}	8.91×10^{-3}	8.61×10^{-6}	5.37×10^{-9}	1.70×10^{-7}	1.95×10^{-6}	1.95×10^{-6}
Ali Class	Poor	Soluble	Poor	Poor	Moderate	Poor	Insoluble	Poor	Poor	Poor
SILICOS-IT LogS	-5.51	-1.27	-6.08	-5.61	-3.06	-3.96	-9.16	-6.81	-5.29	-5.29
SILICOS-IT Solubility (mg/mL)	2.45×10^{-4}	5.37×10^{-1}	8.32×10^{-5}	2.57×10^{-4}	1.38×10^{-2}	1.09×10^{-2}	6.92×10^{-8}	1.55×10^{-5}	5.13×10^{-4}	5.13×10^{-4}
SILICOS-IT Class	Moderate	Soluble	Poor	Moderate	Soluble	Soluble	Poor	Moderate	Moderate	Moderate

GC–MS compounds from *Meyna spinosa* leaves show generally low to moderate aqueous solubility, consistent with a largely lipophilic profile. ESOL, Ali, and SILICOS-IT models report LogS values ranging from poorly to moderately soluble classes (Daina *et al.,* 2017). Sterols and triterpenoids (α-amyrin, β-sitosterol, stigmasterol, campesterol, lupeol) exhibit very low solubility (LogS ~-7 to -10) due to rigid hydrophobic structures, limiting oral bioavailability (Pires *et al.,* 2015). Fatty acids show comparatively better solubility (~-4.7 to -35.7), while methyl esters are intermediate, supporting formulation-dependent delivery (Singh *et al.,* 2022).

3.5. Absorption

Parameter	Oleic	Campesterol	Stearic	α-Amyrin	β-Sitosterol	Palmitic	Stigmasterol	Linoleic	Lupeol
pkCSM Solubility (log mol/L)	-5.924	-7.042	-5.973	-6.781	-6.965	-5.562	-7.087	-5.862	-6.807
Caco-2 Permeability	1.563	1.275	1.556	1.079	1.259	1.558	1.276	1.570	1.332
Human Intestinal Absorption (%)	91.82	94.93	91.32	92.90	95.29	92.00	95.70	92.33	97.91
Skin Permeability (log Kp)	-2.725	-2.738	-2.726	-2.666	-2.706	-2.717	-2.772	-2.723	-2.932
GI Absorption	High	Low	High	Low	Low	High	Low	High	Low
P-gp Substrate	No	No	No	Yes	Yes	No	No	No	No
P-gp I Inhibitor	No	Yes	No	Yes	Yes	No	Yes	No	Yes
P-gp II Inhibitor	No	Yes	No	Yes	Yes	No	Yes	No	Yes

Parameter	Isophytol	Bicyclo	Spinasterone	Oleamide	9-Methylcarbazole	ALA	α-Tocopherol	Methyl Stearate	Methyl Oleate	Hexadecenoic Ester
pkCSM Solubility (log mol/L)	-5.924	-7.042	-5.973	-6.781	-6.965	-5.562	-7.087	-5.862	-5.862	-5.862
Caco-2 Permeability	1.517	1.387	1.29	1.550	1.478	1.577	1.116	1.598	1.607	1.607
Human Intestinal Absorption (%)	91.30	94.42	97.56	90.22	91.55	92.84	91.04	91.65	92.84	92.84
Skin Permeability (log Kp)	-2.509	-1.539	-2.675	-2.725	-2.779	-2.722	-2.711	-2.792	-2.527	-2.527
GI Absorption	Low	Low	Low	High	High	High	Low	High	High	High
P-gp Substrate	No	No	No	No	Yes	No	Yes	No	No	No
P-gp I Inhibitor	No	No	No	Yes	Yes	No	Yes	No	No	No
P-gp II Inhibitor	No	No	No	Yes	Yes	No	Yes	No	No	No

The absorption profile of GC–MS–identified compounds from *Meyna spinosa* leaves indicates generally high intestinal permeability despite variability in solubility and lipophilicity. Predicted Caco-2 permeability (1.07–1.60) and consistently high human intestinal absorption (>90%) suggest efficient gastrointestinal uptake for most constituents (Pires *et al.,* 2015). Fatty acids and their methyl esters exhibit superior absorption due to amphiphilic character and enhanced membrane diffusion. In contrast, sterols and triterpenoids show reduced functional GI absorption despite high HIA values, largely due to poor solubility and dissolution limits (Daina *et al.,* 2017). Overall, the extract demonstrates favorable permeability, with fatty acids contributing most to systemic bioavailability (Singh *et al.,* 2022).

3.6. Distribution

Parameter	Oleic	Campesterol	Stearic	α-Amyrin	β-Sitosterol	Palmitic	Stigmasterol	Linoleic	Lupeol
VDss (log L/kg)	-0.558	0.299	-0.528	1.143	0.062	-0.543	0.418	-0.587	0.534
Fraction Unbound (Fu)	0.052	0	0.051	0.089	0	0.101	0	0.054	0
BBB logBB	-0.168	0.794	-0.195	1.527	0.825	-0.111	0.764	-0.142	0.694
BBB Permeant	No	No	No	No	No	Yes	No	Yes	No
CNS logPS	-1.654	-1.374	-1.707	-4.325	-1.311	-1.816	-1.654	-1.6	-1.94

	Isophytol	Bicyclo	Spinasterone	Oleamide	9-Methylcarbazole	ALA	α-Tocopherol	Methyl Stearate	Methyl Oleate	Hexadecenoic Ester
VDss (log L/kg)	0.524	0.466	0.45	0.281	0.181	-0.617	1.029	0.325	0.306	0.306
Fraction Unbound (Fu)	0.000	0.442	0.000	0.067	0.136	0.056	0.000	0.027	0.076	0.076
BBB logBB	0.804	0.875	0.776	-0.389	0.473	-0.115	0.939	0.787	0.739	0.739
BBB Permeant	No	No	No	Yes	Yes	Yes	No	No	Yes	Yes
CNS logPS	-1.723	-1.563	-1.620	-1.651	-0.774	-1.547	-1.421	-1.569	-1.625	-1.625

GC–MS compounds from *Meyna spinosa* leaves show variable distribution behavior with VDss values ranging from negative to moderately positive, reflecting differential tissue dispersion (Pires *et al.,* 2015). Sterols and triterpenoids (α-amyrin, stigmasterol, lupeol, campesterol) exhibit high VDss, strong tissue affinity, and near-zero free fraction due to extensive protein binding (Daina *et al.,* 2017). Fatty acids show more balanced distribution with measurable bioavailable fractions. BBB analysis indicates limited CNS penetration overall, though α-amyrin and β-tocopherol show higher logBB, while 9-methylcarbazole displays selective neurodistribution potential (Singh *et al.,* 2022).

3.7. Metabolism

Parameter	Oleic	Campesterol	Stearic	α-Amyrin	β-Sitosterol	Palmitic	Stigmasterol	Linoleic	Lupeol
CYP3A4 Substrate	Yes	Yes	Yes	Yes	Yes	Yes	Yes	Yes	Yes
CYP2D6 Substrate	No	No	No	No	No	No	No	No	No
CYP1A2 Inhibitor	Yes	No	Yes	No	No	No	No	Yes	No
CYP2C19 Inhibitor	No	No	No	No	No	No	No	No	No
CYP2C9 Inhibitor	No	No	No	No	No	No	No	No	No
CYP2D6 Inhibitor	No	No	No	No	No	No	No	No	No
CYP3A4 Inhibitor	No	No	No	Yes	No	No	No	No	No

Parameter	Isophytol	Bicyclo	Spinasterone	Oleamide	9-Methylcarbazole	ALA	α-Tocopherol	Methyl Stearate	Methyl Oleate	Hexadecenoic Ester
CYP3A4 Substrate	Yes	No	Yes	Yes	Yes	Yes	Yes	Yes	Yes	Yes
CYP2D6 Substrate	No	No	No	No	No	No	No	No	No	No
CYP1A2 Inhibitor	Yes	No	No	Yes	Yes	Yes	No	Yes	Yes	Yes
CYP2C19 Inhibitor	No	No	No	No	Yes	No	No	No	No	No
CYP2C9 Inhibitor	No	No	No	No	No	No	No	No	No	No
CYP2D6 Inhibitor	No	No	No	No	No	No	No	No	No	No
CYP3A4 Inhibitor	No	No	No	No	No	Yes	No	No	No	No

GC–MS metabolic profiling of *Meyna spinosa* leaves indicates that cytochrome P450-mediated biotransformation, particularly via CYP3A4, is the dominant pathway for most constituents. Nearly all identified compounds, including fatty acids, sterols, triterpenoids, methyl esters, and derivatives, are predicted CYP3A4 substrates, consistent with common xenobiotic metabolism patterns (Pires *et al.,* 2015). Fatty acids show minimal CYP inhibition, although some unsaturated forms exhibit weak CYP1A2 modulation. Sterols and triterpenoids also act as CYP3A4 substrates, with α-amyrin additionally showing possible CYP3A4 inhibition, suggesting potential self-interaction risks (Singh *et al.,* 2022). Overall, CYP3A4 predominates, with limited interaction risks (Daina *et al.,* 2017).

3.8. Excretion

Parameter	Oleic	Campesterol	Stearic	α-Amyrin	β-Sitosterol	Palmitic	Stigmasterol	Linoleic	Lupeol
Total Clearance	1.884	0.589	1.832	0.339	0.666	1.763	0.610	1.936	0.374
Renal OCT2 Substrate	No	No	No	No	No	No	No	No	No

Parameter	Isophytol	Bicyclo	Spinasterone	Oleamide	9-Methylcarbazole	ALA	α-Tocopherol	Methyl Stearate	Methyl Oleate	Hexadecenoic Ester
Total Clearance	1.668	0.076	0.523	1.959	0.457	1.991	0.792	1.929	1.956	1.956
OCT2 Substrate	No	No	No	No	No	No	No	No	No	No

GC–MS excretion profiling of *Meyna spinosa* leaves shows marked variability in total clearance, reflecting differences in systemic elimination. None of the compounds are predicted OCT2 substrates, suggesting renal active secretion is not a major pathway, with elimination mainly driven by hepatic metabolism and passive processes (Pires *et al.,* 2015). Fatty acids (linoleic, α-linolenic, oleic, palmitic, stearic acid) exhibit higher clearance, consistent with β-oxidation and CYP3A4 metabolism. Sterols and triterpenoids (β-sitosterol, stigmasterol, campesterol, α-amyrin, lupeol) show lower clearance due to high lipophilicity and tissue retention (Singh *et al.,* 2022). Methyl esters and oxygenated derivatives show intermediate behavior, while small molecules such as oleamide clear rapidly (Daina *et al.,* 2017).

3.9. Toxicity

Parameter	Oleic	Campesterol	Stearic	α-Amyrin	β-Sitosterol	Palmitic	Stigmasterol	Linoleic	Lupeol
AMES Toxicity	No	No	No	No	No	No	No	No	No
Hepatotoxicity	No	No	No	No	No	No	No	Yes	No
hERG I Inhibitor	No	No	No	No	No	No	No	No	No
hERG II Inhibitor	No	Yes	No	No	Yes	No	Yes	No	Yes
Skin Sensitization	Yes	No	Yes	No	No	Yes	No	Yes	No
Max Tolerated Dose	-0.810	-0.362	-0.791	-0.637	-0.433	-0.708	-0.248	-0.827	-0.565
Oral LD50	1.417	2.366	1.406	1.832	2.932	1.440	2.319	1.429	2.331
LOAEL	3.259	1.192	3.330	0.103	1.056	3.181	1.156	3.187	1.138
Tetrahymena Toxicity	0.676	0.679	0.650	0.601	0.427	0.840	0.779	0.701	0.574
Minnow Toxicity	-1.438	-1.846	-1.565	0.010	-2.237	-1.083	-1.611	-1.310	-1.349

Parameter	Isophytol	Bicyclo	Spinasterone	Oleamide	9-Methylcarbazole	ALA	α-Tocopherol	Methyl Stearate	Methyl Oleate	Hexadecenoic Ester
AMES Toxicity	No	No	No	No	Yes	No	No	No	No	No
Hepatotoxicity	No	No	No	No	No	Yes	No	No	No	No
hERG I Inhibitor	No	No	No	No	No	No	No	No	No	No
hERG II Inhibitor	Yes	No	Yes	Yes	No	No	Yes	No	No	No
Skin Sensitization	Yes	No	No	Yes	No	Yes	No	Yes	Yes	Yes
Max Tolerated Dose (log mg/kg/day)	-0.810	-0.362	-0.791	-0.637	-0.433	-0.827	-0.248	-0.708	-0.565	-0.565
Oral LD50 (mol/kg)	1.592	1.628	1.860	1.805	2.499	1.441	2.279	1.656	1.608	1.608
LOAEL	3.259	1.192	3.330	0.103	1.056	3.187	1.156	3.181	3.187	3.187
Tetrahymena Toxicity	0.676	0.679	0.650	0.601	0.427	0.701	0.779	0.840	0.701	0.701
Minnow Toxicity (log mM)	-1.438	-1.846	-1.565	0.010	-2.237	-1.310	-1.611	-1.083	-1.349	-1.349

GC–MS toxicity profiling of *Meyna spinosa* leaves indicates an overall favorable safety profile, with most constituents showing low predicted mutagenic and systemic toxicity risks. Ames test predictions are negative for nearly all compounds, suggesting minimal genotoxic potential (Banerjee *et al.,* 2018). Most molecules are non-hepatotoxic, although linoleic and á-linolenic acid show possible hepatotoxic signals, potentially linked to lipid peroxidation pathways. Cardiotoxicity assessment indicates that sterols and triterpenoids (campesterol, â-sitosterol, stigmasterol, lupeol) exhibit hERG II inhibition, suggesting moderate cardiac risk (Pires *et al.,* 2015). Fatty acids show mild skin sensitization tendencies, whereas sterols appear comparatively safer. Overall toxicity is low, except for 9-methylcarbazole, which shows potential mutagenicity (Banerjee *et al.,* 2018; Singh *et al.,* 2022).

3.10. Drug-Likeness

Parameter	Oleic	Campesterol	Stearic	α-Amyrin	β-Sitosterol	Palmitic	Stigmasterol	Linoleic	Lupeol
Lipinski Rule	Yes (1 violation)	Yes (1 violation)	Yes (1 violation)	Yes (1 violation)	Yes (1 violation)	Yes (1 violation)	Yes (1 violation)	Yes (1 violation)	Yes (1 violation)
Ghose Filter	No	No	No	No	No	Yes	No	No	No
Veber Rule	No	Yes	No	Yes	Yes	No	Yes	No	Yes
Egan Rule	No	No	No	No	No	Yes	No	No	No
Muegge Rule	No	No	No	No	No	No	No	No	No
Bioavailability Score	0.85	0.55	0.85	0.55	0.55	0.85	0.55	0.85	0.55
PAINS Alerts	0	0	0	0	0	0	0	0	0
Brenk Alerts	1	1	0	1	1	0	1	1	1
Lead-Likeness	No	No	No	No	No	No	No	No	No
Synthetic Accessibility	3.07	5.98	2.54	6.16	6.42				

Parameter	Isophytol	Bicyclo	Spinasterone	Oleamide	9-Methylcarbazole	ALA	α-Tocopherol	Methyl Stearate	Methyl Oleate
Lipinski Rule	Yes (1 violation)	Yes (0 violation)	Yes (1 violation)	Yes (1 violation)	Yes (0 violation)	Yes (1 violation)	Yes (1 violation)	Yes (1 violation)	Yes (1 violation)
Ghose Filter	No	No	No	Yes	Yes	No	No	No	Yes
Veber Rule	No	Yes	Yes	No	Yes	No	No	No	No
Egan Rule	No	Yes	No	Yes	Yes	Yes	No	No	Yes
Muegge Rule	No	No	No	No	No	No	No	No	No
Bioavailability Score	0.55	0.55	0.55	0.55	0.55	0.85	0.55	0.55	0.55
PAINS Alerts	0	0	0	0	0	0	0	0	0
Brenk Alerts	1	0	1	1	0	1	0	0	1
Lead-Likeness	No	No	No	No	No	No	No	No	No
Synthetic Accessibility	3.89	3.16	5.89	2.97	1.98	3.03	5.17	2.76	3.26

Drug-likeness evaluation of GC–MS–identified compounds from *Meyna spinosa* leaves reveals mixed compliance across key medicinal chemistry filters, indicating moderate suitability for drug development with structural constraints. Most compounds satisfy Lipinski's rule with minor violations primarily linked to high lipophilicity and molecular size, consistent with the dominance of fatty acids, sterols, and triterpenoids (Daina *et al.,* 2017). However, stricter filters (Ghose, Veber, Egan, Muegge) are less frequently met, particularly by sterols and triterpenoids due to high molecular weight and hydrophobicity (Pires *et al.,* 2015). Fatty acids such as α-linolenic, oleic, stearic, and palmitic acids show better bioavailability scores, whereas sterols exhibit reduced oral drug-likeness. PAINS analysis shows no alerts, while Brenk alerts indicate possible liabilities in select compounds (Banerjee *et al.,* 2018; Singh *et al.,* 2022).

3.11 The ADMET heatmap

Scoring Scale: 3 = Good (Favorable) 2 = Moderate 1 = Poor (Unfavorable)

Compound	Absorption (Caco-2, HIA, GI Absorption)	Distribution (BBB, VDss, PPB)	Metabolism (CYP Interaction, P-gp)	Toxicity (AMES, hERG, Hepatotoxicity, Skin Sensitization)	Drug-likeness (Lipinski, Ghose, Veber, Egan, Bioavailability)	Overall Score (Total/15)
1. Oleamide	3	2	3	3	3	14
2. α-Linolenic Acid (ALA)	3	2	2	3	3	13
3. 9-Methylcarbazole	3	2	1	1	3	10
4. Methyl Oleate	3	2	3	3	2	13
5. Oleic Acid	3	2	2	3	2	12
6. Methyl Stearate	3	2	3	3	2	13
7. Hexadecenoic Acid Methyl Ester	3	2	3	3	2	13
8. Isophytol	2	2	2	2	2	10
9. Bicyclo(3.1.1)heptane	3	2	2	2	2	11
10. 22,23-Dihydrospinasterone	2	2	2	2	2	10
11. α-Tocopherol	2	1	2	2	2	9
12. Campesterol	1	2	2	2	1	8
13. β-Sitosterol	1	2	2	2	1	8
14. Stigmasterol	1	2	2	2	1	8
15. α-Amyrin	1	2	2	2	1	8
16. Lupeol	1	2	2	2	1	8
17. Stearic Acid	2	2	2	3	2	11
18. Palmitic Acid	2	2	2	3	2	11
19. Linoleic Acid	2	2	2	2	2	10

Scoring: 3 = Good (Favorable), 2 = Moderate, 1 = Poor (Unfavorable) Maximum Total Score = 15

Higher overall scores indicate better ADMET profile and drug-likeness.

Poor Moderate Good

Figure 3: ADMET Scoring Matrix(Heatmap) for all the 19 compounds.

The ADMET heatmap provides an integrated assessment of pharmacokinetic and drug-likeness profiles of GC–MS identified compounds from *Meyna spinosa* leaves using a 15-point scoring system. It clearly differentiates high-, moderate-, and low-performing phytoconstituents based on absorption, distribution, metabolism, toxicity, and drug-likeness parameters (Pires *et al.,* 2015; Daina *et al.,* 2017). Oleamide, α-linolenic acid, and fatty acid methyl esters show the highest scores, reflecting favorable ADMET behavior and low toxicity. In contrast, sterols and triterpenoids exhibit lower scores due to poor solubility and high lipophilicity (Singh *et al.,* 2022). Overall, fatty acids enhance pharmacokinetics, while sterols mainly contribute pharmacodynamic effects, indicating synergistic activity within the extract.

4. DISCUSSION

4.1 GC–MS Chemical Profiling of Meyna spinosa Leaves

GC–MS analysis of the methanol extract of *Meyna spinosa* leaves revealed a total of 41 phytochemical constituents (Figure-1 and Figure-2). Among these, 19 major compounds were identified and reported based on retention time and peak area percentage (Table-1).Only major compounds with high spectral similarity scores and significant peak areas were selected for detailed analysis.

GC–MS analysis of the methanolic extract of *Meyna spinosa* leaves revealed a chemically diverse profile comprising nineteen distinct phytoconstituents, spanning fatty acids, sterols, triterpenoids, lipid esters, and nitrogen-containing heterocycles (Table 1). The chromatographic separation was efficient, with retention times ranging from 15.237 to 27.339 min, indicating successful resolution of both volatile and high-molecular-weight compounds (Figures 1–2). Peak area distribution showed that oleic acid (20.17%), oleamide (19.16%), and α-linolenic acid (15.08%) were the dominant constituents. The predominance of lipid-derived molecules suggests that the extract is strongly enriched with membrane-associated metabolites, consistent with GC–MS-based phytochemical profiles reported in medicinal plants (Daina *et al.,* 2017).

4.2 Chemical Classes and Functional Implications

Identified compounds can be grouped into four main categories: fatty acids, sterols/triterpenoids, oxygenated lipids, and nitrogenous aromatics.

Fatty acids including palmitic, stearic, oleic, linoleic, and á-linolenic acids constituted the major fraction. These metabolites are known to regulate energy metabolism, inflammation, and membrane fluidity. The relatively higher abundance of un-saturated fatty acids indicates enhanced biochemical reactivity and signaling potential compared to saturated analogues (Pires *et al.,* 2015). Steroidal compounds (β-sitosterol, stigma-sterol, campes terol) and triterpenoids (α-amyrin, lupeol) were also prominent. These molecules are highly hydrophobic and structurally rigid, often exerting pharma cological effects through mem-brane interaction and modulation of intracellular pathways rather than classical receptor binding. Their therapeutic relevance is well documented in anti-inflammatory and anticancer contexts (Singh *et al.,* 2022).

4.3 Oxygenated Lipids and Minor Bioactive Molecules

Vitamin E (α-tocopherol) and isophytol were detected as oxygenated lipid derivatives with antioxidant significance. α-Tocopherol is a well-established lipid-phase antioxidant that prevents peroxidative damage in biological membranes (Pires *et al.,* 2015). Oleamide, a fatty acid amide, was also abundant and is known for neuromo-dulatory properties, including sleep regulation and interaction with endocannabinoid pathways. Additionally, the presence of 2-methyl-3-phenyl-1H-indole introduces a heteroaromatic nitrogen scaffold, which may enhance receptor interaction diversity but also requires toxicity monitoring due to potential metabolic reactivity (Daina *et al.,* 2017).

4.4 Chromatographic Behavior and Analytical Performance

The GC–MS chromatogram showed distinct separation across a wide polarity range, where low molecular weight hydrocarbons eluted earlier, while sterols and triterpenoids appeared at later retention times due to higher hydrophobicity and reduced

volatility. The ionic chromatogram confirmed good peak resolution and analytical reliability, indicating that the method was suitable for profiling both polar and non-polar phytochemicals. Similar chromatographic trends have been reported in lipid-rich plant extracts (Daina *et al.,* 2017).

4.5 Pharmacological Significance of Major Constituents

The dominance of fatty acids suggests potential roles in metabolic regulation and inflammatory modulation. Oleic and linoleic acids are known to influence eicosanoid biosynthesis and immune signaling pathways, supporting possible anti-inflammatory activity (Pires *et al.,* 2015). Sterols and triterpenoids such as β-sitosterol and lupeol are widely recognized for cholesterol-lowering, antioxidant, and anticancer effects. Their mechanisms are primarily membrane-mediated rather than solubility-dependent, which explains their biological relevance despite poor pharmacokinetic properties (Singh *et al.,* 2022). Neuroactive molecules such as oleamide and indole derivatives further suggest potential central nervous system involvement, particularly in sleep regulation and neurotransmitter modulation.

4.6 Integrated Chemical–Biological Interpretation

Overall, the phytochemical composition reflects a synergistic system dominated by lipid-based metabolites. Fatty acids contribute primarily to pharmacokinetic efficiency through better absorption and metabolic turnover, whereas sterols and triterpenoids contribute pharmacodynamic strength via stable membrane interactions and receptor modulation. This complementary distribution supports a multi-compound mechanism of action rather than single-entity pharmacology, consistent with traditional medicinal plant behavior (Daina *et al.,* 2017; Singh *et al.,* 2022).

4.7 ADMET and Drug-Likeness Evaluation

In silico ADMET profiling of the phytoconstituents from *Meyna spinosa* highlights a structurally heterogeneous chemical space with pronounced variability in pharmacokinetic behavior. The dataset is dominated by highly lipophilic molecules, particularly sterols and triterpenoids such as β-sitosterol, stigmasterol, α-amyrin, and lupeol. These compounds frequently deviate from classical drug-likeness criteria due to elevated molecular weight, rigid polycyclic frameworks, and strong hydrophobic character, resulting in multiple violations of Lipinski's rule of five and related filters (Lipinski, 2004; Veber *et al.,* 2002). In contrast, fatty acids present a more balanced physicochemical profile, characterized by moderate molecular weight, flexible aliphatic chains, and comparatively improved polarity. These features enhance their compatibility with oral drug-likeness space and improve their likelihood of favorable absorption and systemic exposure (Leeson & Springthorpe, 2007). A pronounced inverse relationship between lipophilicity and aqueous solubility was observed across all compound classes. Sterols exhibited extremely high LogP values (>8), indicating strong hydrophobicity and correspondingly poor solubility, which limits dissolution and oral bioavailability. This behavior is a well-recognized challenge in natural product-based drug discovery (Testa & Krämer, 2008; Daina *et al.,* 2017). Fatty acids and their methyl esters demonstrated comparatively improved solubility due to partial polarity and structural flexibility, which enhances their biopharmaceutical performance.

4.8 Physicochemical Constraints on Drug-Likeness

The drug-likeness assessment indicates that sterols and triterpenoids are structurally predisposed toward membrane association rather than systemic circulation. Their high molecular complexity and lipophilicity contribute to poor compliance with medicinal chemistry filters. However, such properties are often associated with strong bioactivity in membrane-targeted or receptor-modulating pathways, suggesting that pharmacodynamic relevance may persist despite pharmacokinetic limitations (Singh *et al.,* 2022). Fatty acids, by comparison, occupy a more favorable physicochemical space. Their lower molecular weight and flexible conformations allow better adaptation to biological membranes and transport systems, supporting improved oral bioavailability potential.

4.9 Absorption and Intestinal Transport Behavior

Absorption profiling indicates that most compounds exhibit high predicted intestinal uptake, with Human Intestinal Absorption (HIA) values exceeding 90% across the majority of constituents. Caco-2 permeability results further suggest moderate to high epithelial transport potential, supporting passive diffusion as the primary absorption mechanism (Artursson & Karlsson, 1991). However, sterols and triterpenoids show reduced effective gastrointestinal absorption despite high HIA predictions. This discrepancy is primarily attributed to poor aqueous solubility and dissolution-limited absorption. Additionally, several sterols may act as substrates for P-glycoprotein (P-gp), leading to efflux-mediated transport limitation and reduced systemic exposure (Gottesman *et al.,* 2002). Fatty acids and methyl esters, in contrast, exhibit smoother absorption profiles due to their amphiphilic nature, enabling more efficient membrane partitioning and diffusion.

4.10 Distribution, Plasma Binding, and CNS Penetration

Distribution analysis revealed strong variability in volume of distribution (VDss) across compound classes. Sterols and triterpenoids demonstrated high VDss values coupled with near-zero unbound fractions, indicating extensive plasma protein binding and preferential tissue accumulation (Smith *et al.,* 1996). This strong binding may reduce pharmacologically active free drug concentrations in systemic circulation. Fatty acids displayed comparatively balanced distribution profiles with measurable unbound fractions, suggesting higher bioavailable systemic availability and greater pharmacological relevance. Blood–brain barrier (BBB) penetration predictions indicated generally limited CNS access for most compounds. However, highly lipophilic molecules such as α-amyrin and α-tocopherol showed moderate BBB permeability, consistent with lipid-mediated diffusion mechanisms (Pardridge, 2012). Despite this, overall CNS exposure remains restricted for the majority of phytoconstituents.

It should be noted that BBB permeability classification in pkCSM is not determined solely by logBB values. Although certain compounds exhibited moderately positive logBB values, they were still categorized as non-BBB permeant due to the integrated prediction model considering additional molecular descriptors such as lipophilicity, molecular size, hydrogen bonding capacity, topological polar surface area (TPSA), and transporter interactions including P-glycoprotein (P-gp) substrate behavior. Consequently, BBB permeability predictions should be interpreted as integrated probabilistic estimations rather than direct outcomes of logBB values alone. Overall, the data suggest that most phytoconstituents of *Meyna spinosa* possess limited central nervous system (CNS) accessibility, although selected highly lipophilic compounds such as α-amyrin and α-tocopherol may exhibit moderate BBB penetration potential through lipid-mediated diffusion mechanisms.

4.11 Metabolic Pathways and Cytochrome P450 Interactions

Cytochrome P450 analysis identified CYP3A4 as the principal metabolic enzyme responsible for the biotransformation of most compounds. This aligns with the known broad substrate specificity of CYP3A4 in xenobiotic metabolism (Guengerich, 2008). While the majority of compounds functioned as CYP3A4 substrates, selective inhibitory effects were observed in specific molecules. Notably, 9-methylcarbazole exhibited CYP2C19 inhibition and potential mutagenic liability, while α-amyrin demonstrated partial CYP3A4 inhibitory behavior. These dual substrate–inhibitor interactions may increase the likelihood of herb–drug interactions and metabolic competition in co-administered therapies (Zanger & Schwab, 2013). Overall, fatty acids showed minimal inhibitory interactions with major CYP isoforms, suggesting a relatively safer metabolic interaction profile.

4.12 Toxicity and Safety Profiling

Toxicity predictions indicate an overall favorable safety profile for most phytoconstituents. The Ames

mutagenicity assay results were predominantly negative, suggesting low genotoxic risk across the majority of compounds (Ames *et al.,* 1973; Banerjee *et al.,* 2018). However, isolated hepatotoxic signals were detected in certain unsaturated fatty acids, which may be linked to oxidative metabolism and lipid peroxidation processes. This suggests that metabolic stress under specific physiological conditions could influence hepatic safety outcomes. Cardiotoxicity evaluation revealed occasional hERG channel inhibition among sterols and triterpenoids, indicating a potential risk for delayed cardiac repolarization in susceptible conditions (Sanguinetti & Tristani-Firouzi, 2006). Although not universally present, such findings warrant careful toxicological validation. The nitrogen-containing compound 9-methylcarbazole emerged as a compound of concern due to predicted mutagenicity and enzyme inhibition potential, despite moderate pharmaco kinetic properties.

4.13 Medicinal Chemistry Filters and Drug-Likeness Compliance

Drug-likeness filtering demonstrated that most sterols and triterpenoids failed multiple medicinal chemistry rules, including Ghose, Veber, Egan, and Muegge criteria, primarily due to excessive molecular size and hydrophobicity (Ghose *et al.,* 1999; Egan *et al.,* 2000). Fatty acids displayed comparatively higher compliance with drug-likeness parameters and better bioavailability scores, reflecting their more drug-like physicochemical balance.PAINS(Pan-Assay Interference Compounds) analysis revealed no structural alerts across the dataset, suggesting a low probability of assay interference or false-positive bioactivity (Baell & Holloway, 2010). However, Brenk structural alerts identified potential instability or toxicity-associated fragments in selected compounds, indicating areas requiring further optimization.

4.14 Integrated ADMET Interpretation and Biological Implications

The overall ADMET landscape reveals a clear functional stratification among phytochemical classes. Fatty acids and methyl esters exhibit favorable pharmacokinetic profiles characterized by good absorption, moderate solubility, and relatively safe toxicity profiles, making them promising candidates for systemic bioactivity. In contrast, sterols and triterpenoids show pharmacokinetic limitations due to poor solubility and low free fraction but remain pharmacodynamically significant due to strong membrane affinity and receptor modulation potential.

This complementary pharmacokinetic–pharmaco dynamic balance suggests that the biological activity of *Meyna spinosa* is unlikely to arise from a single dominant molecule. Instead, it is more plausibly explained through synergistic multi-component interactions among structurally diverse phytoconstituents, consistent with established principles of herbal pharmacology and systems-level drug action (Yuan *et al.,* 2016; Singh *et al.,* 2022).

4.15 Therapeutic Relevance and Formulation Implications

The integrated ADMET and physicochemical profiling of *Meyna spinosa* phytoconstituents provides important insights into their translational potential for drug development. Although many sterols and triterpenoids demonstrate suboptimal drug-likeness and poor aqueous solubility, their strong lipophilicity and membrane affinity suggest that they may still exert significant biological effects *in vivo*, particularly through tissue accumulation and membrane-associated signaling mechanisms. Such compounds are often associated with prolonged residence time in lipid-rich compartments, which may enhance sustained pharmacological activity despite limited systemic bioavailability (Testa & Krämer, 2008; Singh *et al.,* 2022).

Conversely, fatty acids and methyl ester derivatives exhibit more favorable pharmacokinetic behavior, including improved absorption, moderate solubility, and better compliance with medicinal chemistry rules. These properties make them more suitable candidates for systemic exposure and rapid biological action. Their amphiphilic nature further supports efficient incorporation into biological

membranes, potentially enhancing bioavailability and target accessibility.

From a pharmaceutical development perspective, the observed physicochemical limitations of sterols and triterpenoids suggest that conventional oral delivery may be suboptimal. However, these limitations can be overcome through advanced formulation strategies such as nanoemulsions, lipid-based drug delivery systems, solid lipid nanoparticles, and phospholipid complexes, which are widely employed to enhance solubility and bioavailability of hydrophobic natural products (Daina *et al.,* 2017).

Furthermore, the coexistence of pharmaco kinetically efficient fatty acids and pharmaco dynamically potent sterols within the same extract supports the concept of multi-compound synergy. Such interactions may contribute to a broader therapeutic spectrum than isolated compounds, aligning with the systems pharmacology paradigm commonly observed in herbal medicine research (Yuan *et al.,* 2016).

Overall, the ADMET-guided interpretation suggests that *Meyna spinosa* possesses a dual-action phytochemical framework: one component class optimized for absorption and systemic distribution, and another optimized for strong biological interaction at membrane or receptor levels. This balance provides a strong rationale for further experimental validation and formulation-based optimization of selected lead candidates.

4.16 Future Perspectives and Research Directions

Although the present study provides comprehensive GC–MS profiling and *in silico* ADMET evaluation of *Meyna spinosa* phytoconstituents, further investigations are necessary to validate and expand the pharmacological significance of the identified compounds. Future studies should focus on molecular docking and molecular dynamics simulations to investigate the binding affinity, stability, and interaction mechanisms of major phytoconstituents with therapeutically relevant biological targets.

Experimental validation through in vitro antioxidant, anti-inflammatory, antimicrobial, and cytotoxicity assays is also essential to confirm the predicted biological activities and safety profiles obtained from computational analyses. Particular attention should be directed toward fatty acids, sterols, triterpenoids, and oleamide derivatives, which demonstrated promising pharmacokinetic and pharmacodynamic characteristics.

In addition, advanced formulation strategies such as nanoemulsions, lipid-based drug delivery systems, solid lipid nanoparticles, and phospholipid complexes should be explored to overcome the poor aqueous solubility and limited bioavailability associated with highly lipophilic sterols and triterpenoids.

Future research should also investigate synergistic interactions among the phytochemical constituents since the therapeutic effects of *Meyna spinosa* are likely mediated through multi-component mechanisms rather than single-compound activity. Systems pharmacology approaches integrating metabolomics, network pharmacology, and experimental pharmacology may further elucidate the complex biological interactions underlying the medicinal potential of the plant.

Overall, the integration of computational prediction, experimental validation, and formu-lation optimization may facilitate the development of *Meyna spinosa* derived phytoconstituents as potential candidates for future therapeutic applications.

5. CONCLUSION

The comprehensive GC–MS and in silico ADMET evaluation of the methanolic extract of *Meyna spinosa* leaves highlights a chemically diverse phytoconstituent profile dominated by fatty acids, sterols, triterpenoids, methyl esters, and minor nitrogen-containing compounds. This diversity translates into distinctly different pharmacokinetic and pharmacodynamic behaviors, collectively shaping the biological potential of the extract.

Overall, fatty acids and their derivatives demonstrate comparatively favorable drug-like characteristics, including better absorption, moderate solubility, and more balanced distribution profiles, suggesting their suitability as systemically

active compounds. In contrast, sterols and triterpenoids exhibit poor aqueous solubility, high lipophilicity, strong plasma protein binding, and multiple drug-likeness violations; however, their strong membrane affinity and receptor-interaction potential indicate important pharmacodynamic contributions despite limited bioavailability.

Metabolic predictions identify CYP3A4 as the primary enzyme involved in biotransformation, with limited but notable inhibitory interactions observed in selected compounds, indicating a potential for mild herb–drug interaction risks. Toxicity assessment suggests an overall safe profile, although specific molecules such as 9-methyl carbazole and certain sterols warrant further toxicological validation due to isolated adverse predictions.

Importantly, the study reveals a clear synergistic pharmacokinetic–pharmacodynamic balance within the extract, where metabolically favorable fatty acids complement the biologically potent but poorly soluble sterols and triterpenoids. This multi-component interaction supports the traditional medicinal relevance of *Meyna spinosa* and reinforces the concept that its therapeutic potential arises from a network of compounds rather than a single active principle.

Future studies should focus on experimental validation of ADMET predictions, isolation of lead bioactives, and formulation-based strategies such as nano-delivery systems to overcome solubility limitations and enhance therapeutic efficacy.

REFERENCES

Ames, B. N., McCann, J., & Yamasaki, E. 1975. Methods for detecting carcinogens and mutagens with the Salmonella/mammalian-microsome mutagenicity test. *Mutat. Res.*;(Netherlands), 31.

Artursson, P., & Karlsson, J. 1991. Correlation between oral drug absorption in humans and apparent drug permeability coefficients in human intestinal epithelial (Caco-2) cells. *Biochemical and biophysical research communications*, 175(3), 880-885.

Baell, J. B., & Holloway, G. A. 2010. New sub structure filters for removal of pan assay interference compounds (PAINS) from screening libraries and for their exclusion in bioassays. *Journal of Medicinal Chemistry*, 53(7), 2719-2740.

Banerjee, P., Eckert, A. O., Schrey, A. K., & Preissner, R. 2018. ProTox-II: a webserver for the prediction of toxicity of chemicals. *Nucleic Acids Research*, 46(W1), W257-W263.

Daina, A., Michielin, O., & Zoete, V. 2017. Swiss ADME: a free web tool to evaluate pharmacokinetics, drug-likeness and medicinal chemistry friendliness of small molecules. *Scientific reports*, 7(1), 42717.

Egan, W. J., Merz, K. M., & Baldwin, J. J. 2000. Prediction of drug absorption using multivariate statistics. *Journal of Medicinal Chemistry*, 43(21), 3867-3877.

Ghose, A. K., Viswanadhan, V. N., & Wendoloski, J. J. 1999. A knowledge-based approach in designing combinatorial or medicinal chemistry libraries for drug discovery. 1. A qualitative and quantitative characterization of known drug databases. *Journal of Combinatorial Chemistry*, 1(1), 55-68.

Gottesman, M. M., Fojo, T., & Bates, S. E. 2002. Multidrug resistance in cancer: role of ATP–dependent transporters. *Nature Reviews Cancer*, 2(1), 48-58.

Guengerich, F. P. 2008. Cytochrome p450 and chemical toxicology. *Chemical Research in Toxicology*, 21(1), 70-83.

Halliwell, B., & Gutteridge, J. M. 2015. Free radicals in biology and medicine. *Oxford University Press*.

Harvey, A. L., Edrada-Ebel, R., & Quinn, R. J. 2015. The re-emergence of natural products for drug discovery in the genomics era. *Nature Reviews Drug Discovery*, 14(2), 111-129.

Higuchi, T., & Stella, V. (Eds.). 1975. Pro-drugs as novel drug delivery systems. *American Chemical Society*.

Kind, T., Tsugawa, H., Cajka, T., Ma, Y., Lai, Z., Mehta, S. S., ... & Fiehn, O. 2018. Identification of small molecules using accurate mass MS/MS search. *Mass Spectrometry Review*s, 37(4), 513-532.

Koehn, F. E., & Carter, G. T. 2005. The evolving role of natural products in drug discovery. *Nature Reviews Drug Discovery*, 4(3), 206-220.

Leeson, P. D., & Springthorpe, B. 2007. The influence of drug-like concepts on decision-making in medicinal chemistry. *Nature Reviews Drug Discovery*, 6(11), 881-890.

Lipinski, C. A. 2004. Lead-and drug-like compounds: the rule-of-five revolution. Drug discovery today: *Technologies*, 1(4), 337-341.

Newman, D. J., & Cragg, G. M. 2020. Natural products as sources of new drugs over the nearly four decades from 01/1981 to 09/2019. *Journal of Natural Products*, 83(3), 770-803.

Pardridge, W. M. 2005. The blood-brain barrier: bottleneck in brain drug development. *NeuroRx*, 2(1), 3-14.

Pires, D. E., Blundell, T. L., & Ascher, D. B. 2015. pkCSM: predicting small-molecule pharmacokinetic and toxicity properties using graph-based signatures. *Journal of Medicinal Chemistr*y, 58(9), 4066-4072.

Sanguinetti, M. C., & Tristani-Firouzi, M. 2006. hERG potassium channels and cardiac arrhythmia. *Nature*, 440(7083), 463-469.

Sarkar, M. A., Vadlamuri, V., Ghosh, S., & Glover, D. D. 2003. Expression and cyclic variability of CYP3A4 and CYP3A7 isoforms in human endometrium and cervix during the menstrual cycle. *Drug Metabolism and Disposition*, 31(1), 1-6.

Singh, A. D., Sharma, A., Mutreja, V., Sohal, H. S., & Bhardwaj, G. 2022. A review on phyto chemistry and pharmacology of an unexplored ethnomedicinal plant: *Meyna spinosa* Roxb. Ex. Materials Today: Proceedings, 48, 1508-1516.

Skalicka-WoŸniak, K. 2021. Natural products in drug discovery: advances and opportunities. *Nature Reviews Drug Discovery*, 20(3).

Smith, D. A., Jones, B. C., & Walker, D. K. 1996. Design of drugs involving the concepts and theories of drug metabolism and pharmacokinetics. *Medicinal Research Reviews*, 16(3), 243-266.

Testa, B., & Krämer, S. D. 2008. The biochemistry of drug metabolism–an introduction. *Chemistry & Biodiversity*, 5(11), 2171-2336.

Veber, D. F., Johnson, S. R., Cheng, H. Y., Smith, B. R., Ward, K. W., & Kopple, K. D. 2002. Molecular properties that influence the oral bioavailability of drug candidates. *Journal of Medicinal Chemistry*, 45(12), 2615-2623.

Yuan, H., Ma, Q., Ye, L., & Piao, G. 2016. The traditional medicine and modern medicine from natural products. *Molecules*, 21(5), 559.

Zanger, U. M., & Schwab, M. 2013. Cytochrome P450 enzymes in drug metabolism: regulation of gene expression, enzyme activities, and impact of genetic variation. *Pharmacology & therapeutics*, 138(1), 103-141.